

Optical orientation and rotation of trapped red blood cells with Laguerre-Gaussian mode

Raktim Dasgupta,* Sunita Ahlawat, Ravi Shankar Verma and Pradeep Kumar Gupta

*Laser Biomedical Applications and Instrumentation Division, Raja Ramanna Centre for
Advanced Technology, Indore-452013, India*

*raktim@rrcat.gov.in

Abstract: We report the use of Laguerre-Gaussian (LG) modes for controlled orientation and rotation of optically trapped red blood cells (RBCs). For LG modes with increasing topological charge the resulting increase in size of the intensity annulus led to trapping of the cells at larger tilt angle with respect to the beam axis and thus provided additional control on the stable orientation of the cells under trap. Further, the RBCs could also be driven as micro-rotors by a transfer of orbital angular momentum from the LG trapping beam having large topological charge or by rotating the profile of LG mode having fractional topological charge.

© 2011 Optical Society of America

OCIS codes: (170.4520) Optical confinement and manipulation; (140.3300) Laser beam shaping; (170.1470) Blood or tissue constituent monitoring.

References and links

1. A. Ashkin, J. M. Dziedzic, J. E. Bjorkholm, and S. Chu, "Observation of a single-beam gradient force optical trap for dielectric particles," *Opt. Lett.* **11**(5), 288–290 (1986).
2. D. V. Petrov, "Raman spectroscopy of optically trapped particles," *J. Opt. A, Pure Appl. Opt.* **9**(8), S139–S156 (2007).
3. S. Rao, Š. Bálint, B. Cossins, V. Guallar, and D. Petrov, "Raman study of mechanically induced oxygenation state transition of red blood cells using optical tweezers," *Biophys. J.* **96**(1), 209–216 (2009).
4. S. Rao, Š. Bálint, L. del Carmen Frias, and D. Petrov, "Polarization Raman study of protein ordering by controllable RBC deformation," *J. Raman* **40**(9), 1257–1261 (2009).
5. M. F. Perutz, "Submicroscopic structure of the red cell," *Nature* **161**(4084), 204–205 (1948).
6. K. Mohanty, S. Mohanty, S. Monajembashi, and K. O. Greulich, "Orientation of erythrocytes in optical trap revealed by confocal fluorescence microscopy," *JBO Lett.* **12**, 060606 (2007).
7. S. C. Grover, R. C. Gauthier, and A. G. Skirtach, "Analysis of the behaviour of erythrocytes in an optical trapping system," *Opt. Express* **7**(13), 533–539 (2000).
8. S. Bayouth, T. A. Nieminen, N. R. Heckenberg, and H. Rubinsztein-Dunlop, "Orientation of biological cells using plane-polarized Gaussian beam optical tweezers," *J. Mod. Opt.* **50**, 1581–1590 (2003).
9. G. Garab, P. Galajda, I. Pomozi, L. Finzi, T. Praznovszky, P. Ormos, and H. van Amerongen, "Alignment of biological microparticles by a polarized laser beam," *Eur. Biophys. J.* **34**(4), 335–343 (2005).
10. S. Sato, M. Ishiguro, and H. Inaba, "Optical trapping and rotational manipulation of microscopic particles and biological cells using higher-order mode Nd-YAG laser beams," *Electron. Lett.* **27**(20), 1831–1832 (1991).
11. R. Dasgupta, S. K. Mohanty, and P. K. Gupta, "Controlled rotation of biological microscopic objects using optical line tweezers," *Biotechnol. Lett.* **25**(19), 1625–1628 (2003).
12. A. T. O'Neil, and M. J. Padgett, "Rotational control within optical tweezers by use of a rotating aperture," *Opt. Lett.* **27**(9), 743–745 (2002).
13. V. Bingelyte, J. Leach, J. Courtial, and M. J. Padgett, "Optically controlled three-dimensional rotation of microscopic objects," *Appl. Phys. Lett.* **82**(5), 829–831 (2003).
14. "BioRyx 200 Applications," <http://www.arrayx.com/PDFdocs/BiorryxApplications.pdf>.
15. S. K. Mohanty, R. Dasgupta, and P. K. Gupta, "Three-dimensional orientation of microscopic objects using combined elliptical and point optical tweezers," *Appl. Phys. B* **81**(8), 1063–1066 (2005).
16. S. K. Mohanty, and P. K. Gupta, "Laser-assisted three-dimensional rotation of microscopic objects," *Rev. Sci. Instrum.* **75**(7), 2320–2322 (2004).
17. S. K. Mohanty, A. Uppal, and P. K. Gupta, "Self-rotation of red blood cells in optical tweezers: prospects for high throughput malaria diagnosis," *Biotechnol. Lett.* **26**(12), 971–974 (2004).
18. S. K. Mohanty, K. S. Mohanty, and P. K. Gupta, "Dynamics of Interaction of RBC with optical tweezers," *Opt. Express* **13**(12), 4745–4751 (2005).

19. J. A. Dharmadhikari, S. Roy, A. K. Dharmadhikari, S. Sharma, and D. Mathur, "Naturally occurring, optically driven, cellular rotor," *Appl. Phys. Lett.* **85**(24), 6048–6050 (2004).
20. J. A. Dharmadhikari, S. Roy, A. K. Dharmadhikari, S. Sharma, and D. Mathur, "Torque-generating malaria-infected red blood cells in an optical trap," *Opt. Express* **12**(6), 1179–1184 (2004).
21. P. Török, and P. R. T. Munro, "The use of Gauss-Laguerre vector beams in STED microscopy," *Opt. Express* **12**(15), 3605–3617 (2004).
22. A. T. O'Neil, and M. J. Padgett, "Axial and lateral trapping efficiency of Laguerre-Gaussian modes in inverted optical tweezers," *Opt. Commun.* **193**(1-6), 45–50 (2001).
23. H. Rouse, *Elementary Mechanics of Fluids, Ch. VIII* (Wiley Eastern Pvt. Ltd, 1970).
24. A. T. O'Neil, I. MacVicar, L. Allen, and M. J. Padgett, "Intrinsic and extrinsic nature of the orbital angular momentum of a light beam," *Phys. Rev. Lett.* **88**(5), 053601 (2002).
25. V. Garcés-Chávez, K. Volke-Sepulveda, S. Chávez-Cerda, W. Sibbett, and K. Dholakia, "Transfer of orbital angular momentum to an optically trapped low-index particle," *Phys. Rev. A* **66**(6), 063402 (2002).
26. H. Ukita, and M. Kanehira, "A Shuttlecock Optical Rotator—Its Design, Fabrication and Evaluation for a Microfluidic Mixer," *IEEE J. Quantum Electron.* **8**(1), 111–117 (2002).
27. S. Maruo, and H. Inoue, "Optically driven viscous micropump using a rotating microdisk," *Appl. Phys. Lett.* **91**(8), 084101 (2007).
28. P. Galajda, and P. Ormos, "Orientation of flat particles in optical tweezers by linearly polarized light," *Opt. Express* **11**(5), 446–451 (2003).
29. M. Khan, S. K. Mohanty, and A. K. Sood, "Optically-driven red blood cell rotor in linearly polarized laser tweezers," *Pramana* **65**(5), 777–786 (2005).
30. J. Leach, E. Yao, and M. J. Padgett, "Observation of the vortex structure of a non-integer vortex beam," *N. J. Phys.* **6**, 71 (2004).
31. S. H. Tao, X.-C. Yuan, J. Lin, X. Peng, and H. Niu, "Fractional optical vortex beam induced rotation of particles," *Opt. Express* **13**(20), 7726–7731 (2005).

1. Introduction

Recently, there has been considerable interest in Raman spectroscopic studies on optically trapped red blood cells (RBCs). This has been motivated by the fact that optical tweezers [1] can immobilize cells in a physiological buffer medium, away from substrate, and thus help avoiding the adverse effects associated with immobilization of cell on the substrate and the contribution of the substrate to the measured spectra of the cell [2]. Because of these advantages, "Raman tweezers", the experimental set-up for recording Raman spectra from an optically trapped cell [2], have been successfully used to carry out several rather interesting experiments like, for example, oxy/deoxy transition in a trapped RBC on application of mechanical stress as would happen in the *in vivo* conditions [3]. Polarized Raman spectroscopic measurements have also been reported and these have provided evidence of increased hemoglobin (Hb) ordering as the RBC is stretched with optical tweezers [4]. Indeed it is believed from quite a long time that intracellular Hb is not randomly distributed, as in free liquid, but exists in a semicrystalline state which is believed to play an important role in intracellular oxygen diffusion [5]. However, to obtain a complete picture of Hb packing, Raman measurement at different polarization configurations including polarization of the Raman excitation beam parallel and normal to the plane of the cell are required. Because the RBC when optically trapped, orients with its plane parallel to the trap beam [6, 7], in order to carry out these measurements, techniques need to be developed for controlling the orientation of optically trapped RBC in the vertical plane, that is the plane containing the trap beam axis. Several optical tweezers based techniques have been used for orientation and rotation of trapped objects [8–16]. Linearly polarized trap beams [8, 9] or trap beams having elliptical intensity distribution [10–12] have been used for orientation of objects, but these can only orient the object in a plane transverse to the laser beam axis. For orientation of trapped object in the vertical plane, one approach is to use two or more closely separated optical traps to hold different parts of the same object. By changing the relative position of these traps the trapped object can be oriented in three dimensions [13, 14]. Other approaches used to orient a trapped object in three dimension are the use of a combination of two trap beams, one having a circular intensity profile and the other with elliptic intensity profile [15], or application of a tangential light forces at the periphery of the trapped object using a pulsed laser beam [16]. All these methods require two or more trap beams leading to some complexity in their

implementation. In this paper we show that a more convenient approach for orientation of trapped RBC is the use of Laguerre-Gaussian (LG) trap beam. Since the LG modes have an annular intensity profile, size of which increases with the azimuthal index or topological charge of the mode, the desired control over the orientation of the trapped RBC in the vertical plane could be achieved with a change in the topological charge of the trapping beam. We also show that another advantage with the use of LG trap beam is that it can transfer its orbital angular momentum to the cell leading to a rotational torque on the cell, which is proportional to the topological charge of the LG beam. Our studies show that at trap beam power of ~ 15 mW, a topological charge of 15 or more provides enough torque to the cell to cause it to rotate in the isotonic buffer medium. Further, we find that LG mode with non-integer topological charge ($l = 0.5$), which possesses a semi circular transverse intensity profile, could also be used for rotating the cells in the trapping plane by rotating the beam pattern. The advantages offered by these approaches over other methods for causing rotation of RBCs [10,11, 17–20] are also discussed.

2. Materials and methods

The experimental set-up consists of a 1064 nm laser source (Compass 1064-4000, Coherent Inc). The laser beam was expanded using the 3X telescopic assembly (L1 and L2) to match the active area of the spatial light modulator (SLM; PLUTO, Holoeye photonics AG, 1920x1080 pixels of size $\sim 8 \mu\text{m} \times 8 \mu\text{m}$). A half wave plate (HWP) was used to make the polarization of the light incident on SLM vertical so that the SLM acts as a pure phase modulator. Each pixel of the SLM can modulate the incoming light in a phase range between 0 and $\sim 2\pi$. For the generation of LG beams the phase profile of the light incident on the SLM was suitably modified using computer generated holograms imprinted on the SLM. The diffracted first order was selected using an iris and directed through mirrors onto the entrance pupil of a water immersion objective lens (Olympus Plan Apochromat 60X, NA 1.2) to form the optical trap. The polarization ellipticity of the trap laser beam was controlled using a polarizer (P) and quarter wave plate (QWP) combination placed after the SLM. For all the experiments left circularly polarized LG modes were used since it leads to symmetric annular intensity distributions at the trap focus [21]. The images and videos of the trapped cells were recorded using a CCD camera (Watec Inc). A filter was used to cut-off the back-scattered laser light.

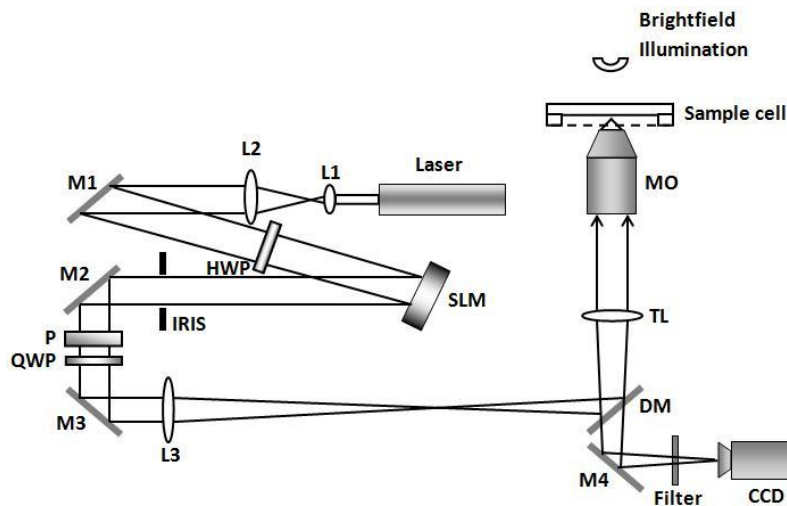


Fig. 1. Experimental set-up. M1 to M4 are the steering mirrors and DM is the dichroic mirror used to selectively reflect the trapping beam onto the entrance pupil of the objective lens.

Blood (1 ml) was collected by venipuncture from healthy volunteers in glass tubes containing EDTA (5.4mg/3ml) as an anticoagulant. RBCs were separated from these anticoagulated blood samples by centrifugation at 600 g for 3 minutes and suspended in phosphate buffer saline (PBS). For experiments appropriate dilutions of the cells in PBS solution was used. In isotonic buffer the shape of the RBCs is that of a biconcave disks (flattened and depressed in the center to result in a dumbbell-shaped cross section) with a diameter of $\sim 7 \mu\text{m}$ and a thickness of $\sim 1.5 \mu\text{m}$ [7].

The circularly symmetric LG laser modes are usually denoted as LG_{pl} where p is the radial index and l is the azimuthal index or topological charge that refers to the number of 2π phase cycles around the circumference of the mode and $(p+1)$ indicates the number of radial nodes in the mode profile. For topological charge greater than zero, the intensity pattern of the LG beam becomes annular. The radius of the annulus is given as [22]

$$r_{\max} = w_0 \sqrt{l/2} \quad (1)$$

where w_0 is the Gaussian beam radius. The LG modes with $l \neq 0$, carry an orbital angular momentum of $l\hbar$ per photon. This is in addition to any angular momentum the light may possess due to its polarization state.

A rotating trapped cell experiences a rotational viscous drag which can be estimated from the following equation [18],

$$T_D = C_D \rho \omega^2 R^5 / 4 \quad (2)$$

For disk shaped cells, the drag coefficient can be expressed as $C_D \approx 24/Re$ [23]. For our case, the Reynolds number is expected to be $\ll 1$ as the rotational frequency is only fraction of Hz, and can be expressed as $Re \approx \rho \omega R^2 / \eta$. Where ρ is the density of the medium, η is the viscosity coefficient on the medium, ω is the rotational speed and R is the average radius of the disk shaped RBC. For a given trap beam power, the maximum rotational speed of a rotating cell will be determined from the balancing action between the light induced torque and the fluid drag.

3. Results and discussions

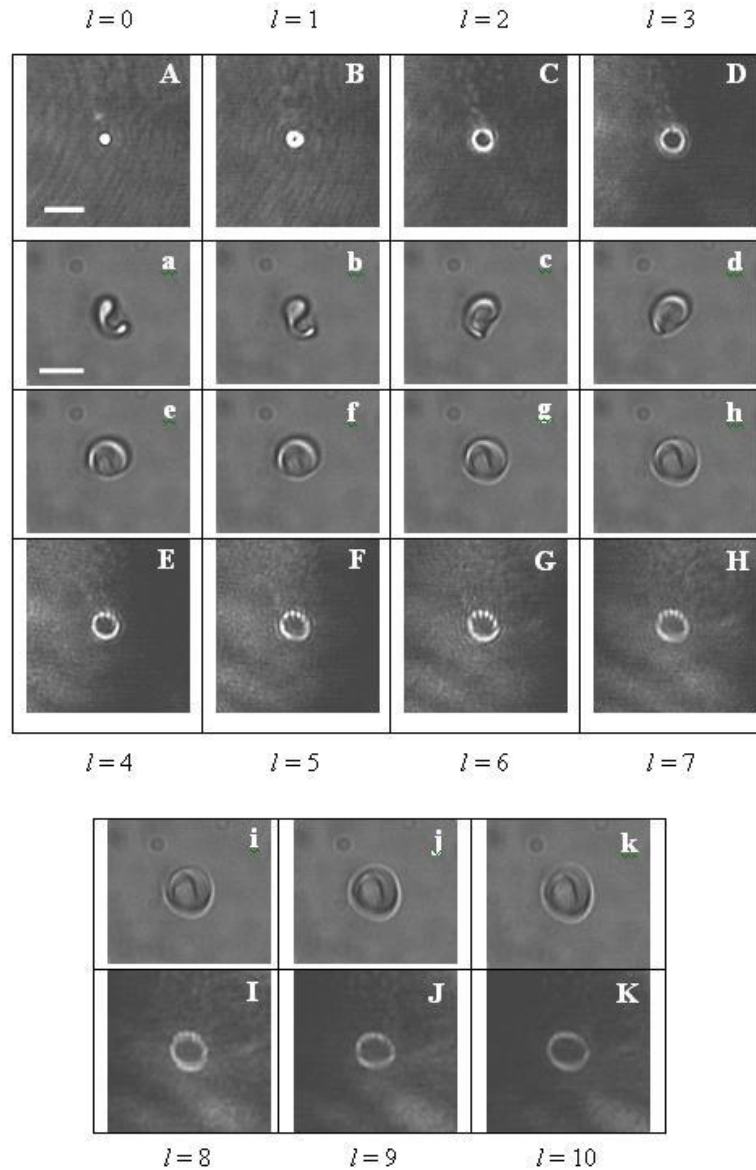


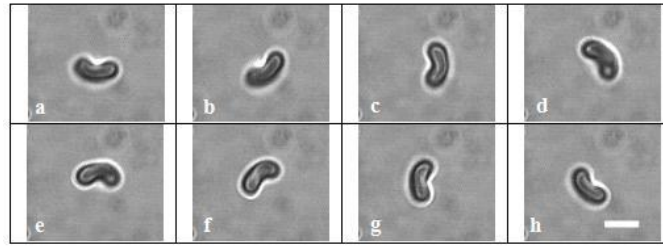
Fig. 2. Image frames from the movies ([Media 1](#) and [Media 2](#)) showing the LG mode patterns from topological charge 0 to 10 (A-K) and the corresponding orientation of a trapped RBC (a-k) respectively. The time interval between consecutive holograms was ~ 0.5 s. Scale bar, 2.5 μm . (A-K) and 6 μm (a-k).

Figure 2 shows the change in the orientation of a trapped RBC with changes in the topological charge of the LG modes. For the zeroth order LG mode (which is identical to TEM_{00}) the cell orients with its plane along the direction of the trapped beam (vertical orientation), since this maximizes the overlap of the cell volume with the region of highest light field. As the size of the bright annulus increases with mode order, maximum overlap between the cell volume and the trapping field is expected for cell orientation away from the vertical direction. For $l=10$ the cell can be seen to be oriented in the horizontal plane that is the trapping plane as this maximizes the overlap of the cell volume with the region of highest light field. For the 1064

nm trap beam the diameter of the bright annulus was estimated to be $\sim 0.8 \mu\text{m}$ for $l = 1$ and $\sim 2.6 \mu\text{m}$ for $l = 10$.

For effecting a change in the orientation of the cell, the optical torque arising due to a change in the mode index of the LG trap beam, should exceed the Brownian forces. An estimate for the resulting optical torque can be obtained by finding the maximum frequency of the change in the mode index from $l = 0$ to 10, up to which the trapped cells could get oriented. It was observed that at a trapping power of $\sim 15 \text{ mW}$, if the mode index is changed at a rate faster than 150 ms between the consecutive modes, the trapped RBC fails to orient. This implies that a time of 1.5 s was required for rotating the cell by 90° from the vertical to horizontal orientation, indicating the maximum rotational speed of $\sim 10 \text{ rpm}$. From Eq. (2) we estimate the corresponding rotational torque, $T_D \sim 0.17 \text{ pN } \mu\text{m}$. The value is two orders of magnitude higher than the random thermal torque ($\sim k_B T$) which at room temperature equals $\sim 10^{-3} \text{ pN } \mu\text{m}$ and therefore ensures stable orientation of the trapped cells by LG trap beam against Brownian forces.

i



ii

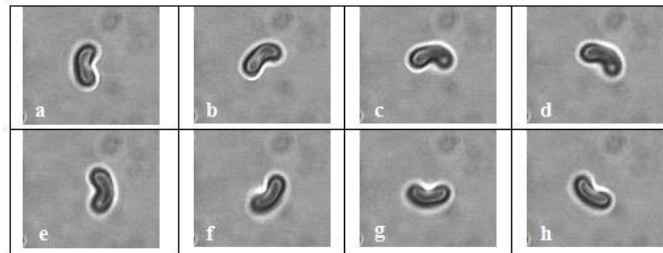


Fig. 3. Image frames from the movie (Media 3) showing the rotation of a trapped RBC via transfer of light orbital angular momentum when trapped under $|l|=15$ mode. The movie shows reversal of the rotational sense as the topological charge of the LG trapping mode was switched from (i) $l=15$ to (ii) $l=-15$. The frames (a-h) show images of the rotating cells, where in each frame the cell is observed to be rotated by an angle of 45° over the previous frame. The time separation between the frames is $\sim 625 \text{ ms}$. Scale bar, $5 \mu\text{m}$. The rotational speed of the cell was $\sim 12 \text{ rpm}$ at $\sim 15 \text{ mW}$ of trap power.

We also observed that the torque exerted by LG trapping beam with high topological charges ($|l| \sim 15$ or more) could drive RBCs as natural micro-rotors. For $|l| \sim 15$ the trapped cells get aligned over the bright annulus of the LG trap due to larger circumference of the annulus. Under such condition the cells while being contained within the annular ring of light, orbits the beam axis in a direction determined by the handedness of the helical phase fronts. This is believed to be due to the transfer of light orbital angular momentum to the trapped cells by the scattering of the trap beam having helical wavefront [24, 25]. Figure 3(i) shows the rotation of an RBC when trapped under $l = 15$ mode. The observed rotational frequency was $\sim 12 \text{ rpm}$ at $\sim 15 \text{ mW}$ of trapping power and it can be increased using higher trap beam power. To check whether the observed rotation is caused by the transferred light orbital angular momentum

from the trap beam to the cell we changed the helicity of the trap beam. Figure 3(ii) shows the corresponding rotation of an RBC when trapped under $l = -15$ mode. The sense of rotation was observed to get reversed that is from counter-clockwise to clockwise direction as the charge of the LG mode was made negative. This allows for a means to change the sense of rotation of a micro-rotor system by simply changing the helicity of the trapping beam. Such control over rotational sense is not possible with techniques utilizing specially fabricated micro-structures [26, 27] or RBCs suspended in hypertonic buffers [17,18]. A control on the sense of rotation can facilitate bi-directional operation for micro-machine components like micro-motors or valves.

It is pertinent to note here that shape anisotropy or birefringence properties of cellular objects could also be exploited for rotation of cells. When inside a hypertonic buffer the RBC's shape becomes asymmetric and can experience rotational torque from the trapping light beam and rotate much like a windmill [17, 18]. Further, as when trapped using linearly or circularly polarized light, birefringent particles get oriented or rotated respectively by transfer of light spin from the trap beam, the birefringence properties of some cellular components like chloroplasts etc have been also exploited to achieve optical rotation [8, 9]. Since with LG trapping modes, the scattering of helical light wavefronts by the trapped cell cause it to rotate, this method is independent of shape anisotropy or birefringence properties of the cell and is more generally applicable to any cell type. We could observe similar transfer of light angular momentum to a leucocyte cell when trapped using $l = 15$ trapping beam (supplementary movie [Media 4](#)). It is also pertinent to note here that when a linearly polarized trap beam is used, due to its shape anisotropy, the vertically oriented RBC gets aligned with its symmetry axis perpendicular to the electric vector of the trapping beam [18,19]. Rotation of the trapped RBC can be effected by rotation of the plane of polarization of the trapping beam by use of a half wave plate, much like what has been demonstrated for micro-disks [28]. To avoid any alignment torque produced by a linearly polarized light beam on trapped cells, we used left circularly polarized $|l| = 15$ trapping beam. With 15 mW of circularly polarized LG ($l = \pm 15$) trap beam we did not observe the cells to spin about their symmetry axis. These results are at variance to the report from Dharmadhikari et al [19, 20] and consistent with results expected from nonbirefringent flat disks [28, 29].

We also observed that rotational drive could be effected onto the trapped RBCs with employment of LG trapping mode having fractional topological charge. The transverse profiles of fractional LG modes are circularly asymmetric and can trap the cells in a preferred orientation. An LG beam with fractional topological charge is distinguished from an integer-order beam in terms of the intensity pattern, which possesses a radial opening (low-intensity gap) in the annular intensity ring encompassing the dark core [30, 31]. Therefore, rotation of the trapping profile makes the trapped cell to rotate. We used LG mode with fractional charge $l=0.5$, that have a nearly semi-circular intensity pattern. Trapped cells orient in the vertical plane with their longer dimension overlapping with that of the trap profile. The LG profile could therefore be rotated by rotation of the generating holographic pattern through SLM. Figure 4 shows the rotation of a trapped RBC using $l = 0.5$ mode. Twenty four consecutive holograms were used to generate the rotating $l = 0.5$ patterns where each pattern is rotated by 15° with respect to the preceding pattern. The rotational speed of the trapped cell could be controlled by changing the time intervals between the holograms displayed on the SLM. At ~ 15 mW of trapping power a rotational speed of up to ~ 18 rpm could be achieved. The rotational frequency can be further increased by increasing the trapping power and also by increasing the step size suitably. The rotational torque corresponding to the maximum speed of 18 rpm could be estimated using Eq. (2) as ~ 0.3 pN μm . Compared to the use of a rotating elliptically profiled trap beam generated using either a first order Hermite Gaussian mode [10] or a cylindrical lens [11] or a rotating aperture [12] the present method avoids insertion of a rotating optical element into the trap beam path and thus the associated alignment problems.

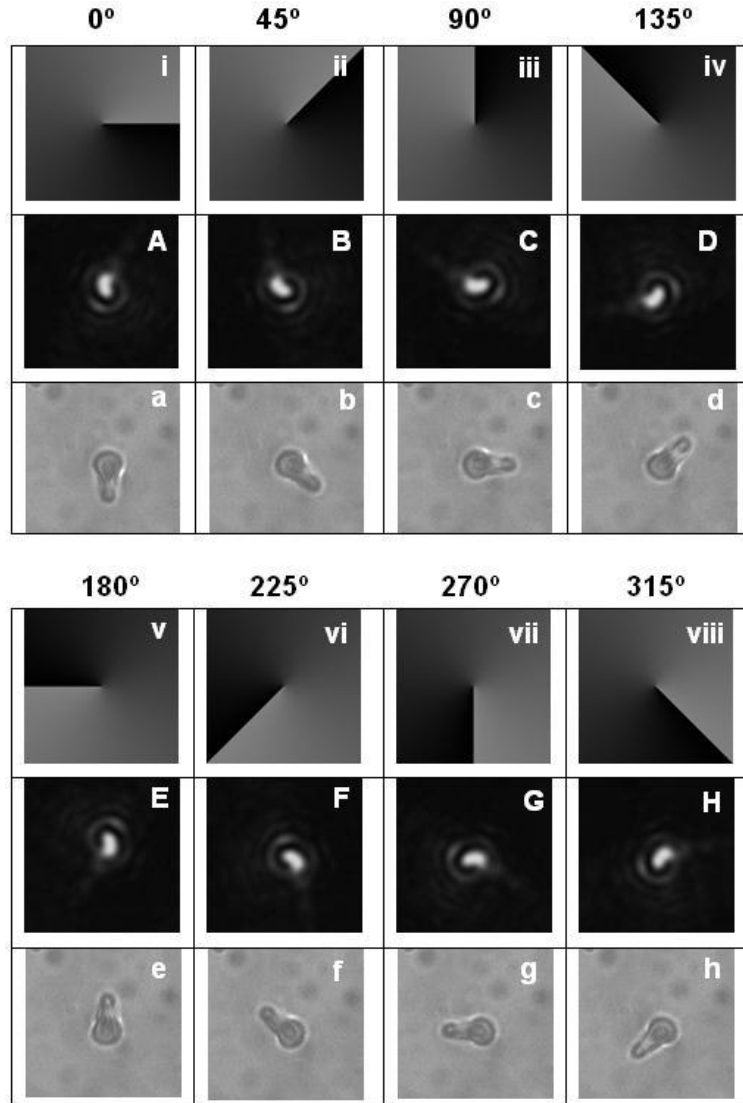


Fig. 4. (i-viii) The computer generated phase holograms encoded in grayscale (256 levels) images. Phase retardation of zero is encoded in black. Gray value 128 represents phase retardation value π . The angles of rotation of the holograms with respect to the first frame are indicated above the corresponding image frames. (A-H) The $l = 0.5$ trapping profiles rotated following the generating hologram patterns. As phase is undefined at the dislocation line the light intensity can be seen to be zero near that region producing an approximate semi-circular profile. (a-h) Image frames from the movie ([Media 5](#)) showing the rotation of an RBC trapped along the longer dimension of the trap profile. The rotational speed of the cell was ~ 15 rpm.

4. Conclusions

We have shown that LG trap beams provide a convenient method for controlled three dimensional orientations of optically trapped RBC. With LG modes having increasing topological charge, the increasing size of the intensity annulus led to trapping of the cells at larger tilt angle with respect to the beam axis and this could be used for controlled orientation of the cell. Such a control on orientation of RBC may help in carrying out polarized Raman spectroscopic measurements on trapped RBCs at all possible polarization configurations. Further, the RBCs could also be driven as micro-rotors by a transfer of orbital angular

momentum from the LG trapping beam having large topological charge and the method also allows for a control in the sense of rotation by reversing the topological charge of the beam. Rotation of the cells by rotating the profile of LG mode having fractional topological charge has been also demonstrated.